Dynamics of Taylor cone formation on surfaces of polymer solutions

L. Vyslouzilova[1], P. Pokorny[1], P. Mikes[1], M. Bilek[2], R. Deliu[3], E. Amler[4,5], M. Buzgo[4,5], V. Vekselman[6], K. G. Kornev[6], D. Lukas[1,7,*]

[1]Faculty of Textile Engineering – Nanoscience Centre, Technical University of Liberec, Studentska 2, Liberec 1, 461 17, Czech Republic.

[2] Faculty of Mechanical Engineering, Technical University of Liberec, Studentska 2, Liberec 1, 461 17, Czech Republic.

[3]Faculty of Textile-Leather and Industrial Management, Technical University "Gh.Asachi", Iassy, Romania, Blvd. Dimitrie Mangeron 53, 700050.

[4] Institute of Biophysics, 2nd Faculty of Medicine, Charles University in Prague, V Uvalu 84, 150 06, 5-Motol, Prague, Czech Republic.

[5] Laboratory of Tissue Engineering, Institute of Experimental Medicine, Academy of Sciences of the Czech Republic, v. v. i., Videnska 1083, Prague, Czech Republic..

[6]School of Material Science and Engineering, Clemson University, USA, Clemson University, 161 Sirrine Hall , Clemson, SC 29634.

[7]Centre for Nanomaterials, Advanced Technologies and Innovation of Technical univerzity of Liberec, Studentska 2, Liberec 1, 461 17, Czech Republic.

[*]The author to whom correspondence should be addressed, david.lukas@tul.cz, tel: 0420485353146

Journal: Physical Review E

Part 2: Nonlinear and Plasma Physics, Fluid Dynamics, and Related Topics - Fluid dynamics

Abstract

We analyze the dynamics of formation of a cone-like protuberance, the Taylor cone, on a free surface of a polymer solution upon application of electric field. The main attention is paid to the quantification of the characteristic time of the Taylor cone formation. This time was experimentally determined by recording the volt-ampere characteristics of the interelectrode gap and filming the evolution of protuberance. Experimental data on aqueous solutions of Poly (vinyl alcohol) with different concentrations appear to be in a good agreement with a theoretical estimate based on the Larmor-Tonks–Frenkel instability theory of the protuberance nucleation.

Key words

Electrohydrodynamics, 47.65.-d, 83.50.Uv, Fluid mechanics, applied, 47.85.-g, Flow instabilities, interfacial, 47.20.Ma, Electrospinning

I. Introduction

Recent progress in nanofiber formation by electrospinning has significantly advanced different fields of materials science and engineering. Electrospun nanofibers and their constructs find applications as materials for tissue engineering and scaffolds (1-3) , for smart textiles (4-7) and for catalysts, solar-cells, and many other applications (8-12).

In electrospinning, a polymer solution is electrically charged by applying a high voltage and the cone-like protuberances appear spontaneously at the liquid-air interface (8, 9, 13). Increasing voltage further, one reaches a moment when the electrostatic force exceeds the surface tension and a protuberance transforms into a spike emanating a jet (8-11, 14-17). The idea of electrospinning from a free liquid surface has led to the development of a special instrument enabling industrial production of nanofibers (18).

The onset of electrospinning from a free liquid surface belongs to a category of the liquid surface instabilities known as the Larmor-Tonks–Frenkel instabilities (19-21). This instability plays a critical role in various scientific, technical, and technological applications, such as electrospraying of liquids, electrogeneration of droplets, and formation of liquid-metal ion sources (22), (23, 24).

In this paper we study the Taylor cone development (22, 25) concentrating our efforts on the physical mechanism of instability development just before the jet emanation. Using aqueous solutions of Poly (vinyl alcohol) (PVA), we study the time of formation of a cone-like protuberance as a function of liquid viscosity. Theoretical interpretation of experimental data has been based on the linear Larmor-Tonks–Frenkel theory of the wave growth when the inertial, capillary, viscous, and electric forces are comparable. We showed that this theory explains the observed experimental data fairy well.

II. Experimental setup

The experimental setup is shown in Fig. 1A, 1B. A metal rod with diameter d = 8 mm and length l = 218 mm was supporting a droplet and was used as an electrode as well. The rod was mounted

on an insulating stand using a three jaw chuck. A flat circular metallic disk of 150 mm in diameter was used as a collector. The rod and disk collector were separated by a gap of thickness L = 100 mm. A 300 Watt High Voltage DC Power Supply (AU-60PO.5-L, Matsusada Precision Inc.) providing the voltage up to 50 kV, and current up to 6 mA was used in these experiments. The rod was connected to the positive pole of the high voltage source, while the collector was grounded. Photographic snapshots of electrospun polymeric droplets were taken using stereopticon Meopta and Nikon camera Coolpix 4500. Surface tension measurements were done using the digital tensiometer (Krűss K9) and viscosity of polymer solutions was obtained using viscometer Haake Roto Visco 1 Thermoscientific at the temperature of 20^{o}C.

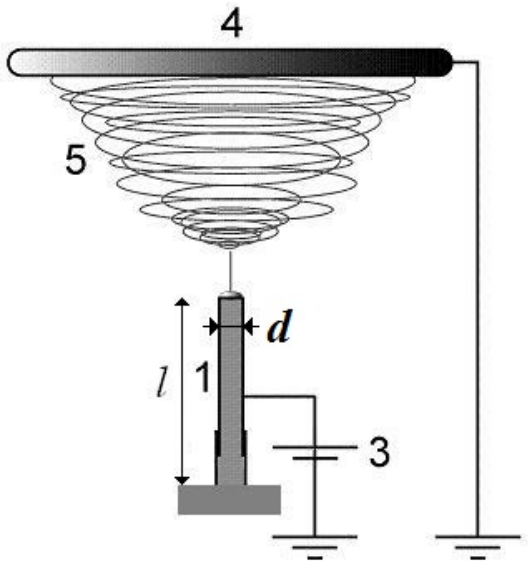

A

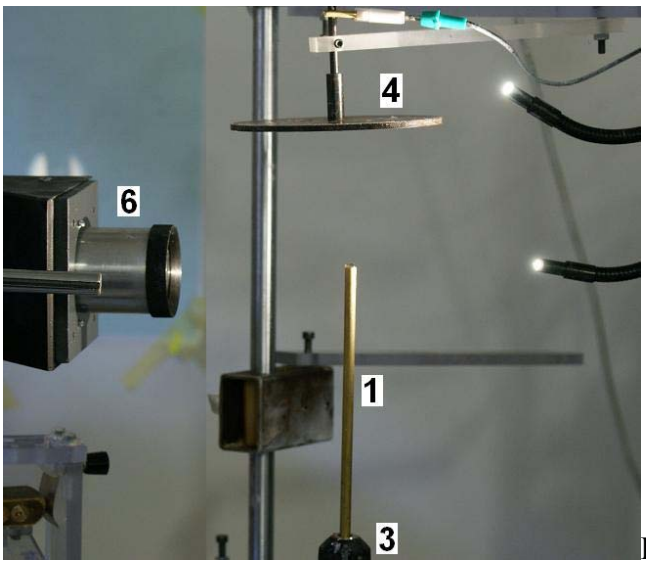

B

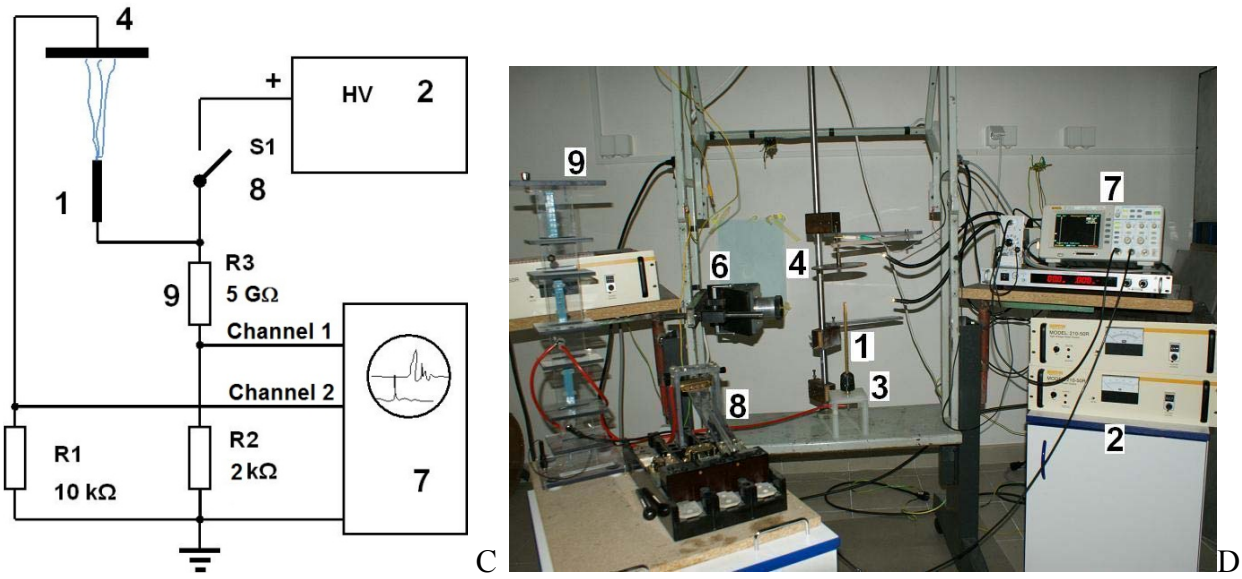

Fig. 1: (A) Schematic of electrospinning setup: the rod electrode (1) is connected to the plus pole of a high voltage source (2). The rod is mounted on an insulating stand using a chuck (3). A vigorously spinning jet (5) hits a circular disk collector (4). (B) Experimental setup, the numbers correspond to schematic A. The stereopticon Meopta is shown as (6). (C) The circuit for measurements of the characteristic time of Taylor cone formation consists of oscilloscope (7), switcher (8) and a voltage divider (9). (D) Experimental setup.

A setup for measurements of characteristic hydrodynamic times is shown in Fig. 1 C It allows one to read two voltaic signals at channels 1 and 2 of the oscilloscope. The channel 1 records the switch-on state of the rod that is triggered by the switch S1. This entry is represented by a lower voltage signal on oscilloscope records depicted in Fig. 2A. Voltage waveforms are recorded at channel 1 of the oscilloscope using voltage divider formed by resistors R3 and R2. The switch point appears as a peak at time t_1. The oscilloscope channel 1 records the voltage on the rod, and hence, on a droplet. The electric current caused by the charges reaching the collector is recorded

at channel 2 of the oscilloscope and appears as a next delayed signal having its peak at time t_2. These charges are formed in the vicinity of the Taylor cone and are accelerated by electric field pushing them toward the collector. The time of ion transport to the counter electrode is measured in milliseconds, hence can be safely neglected here (26). Therefore the time difference $\Delta t = t_2 - t_1$ is defined as the characteristic time of formation of the Taylor cone.

In Fig. 3, we collect the experimental data obtained by this method and compare them with the Larmor-Tonks-Frenkel relaxation times.

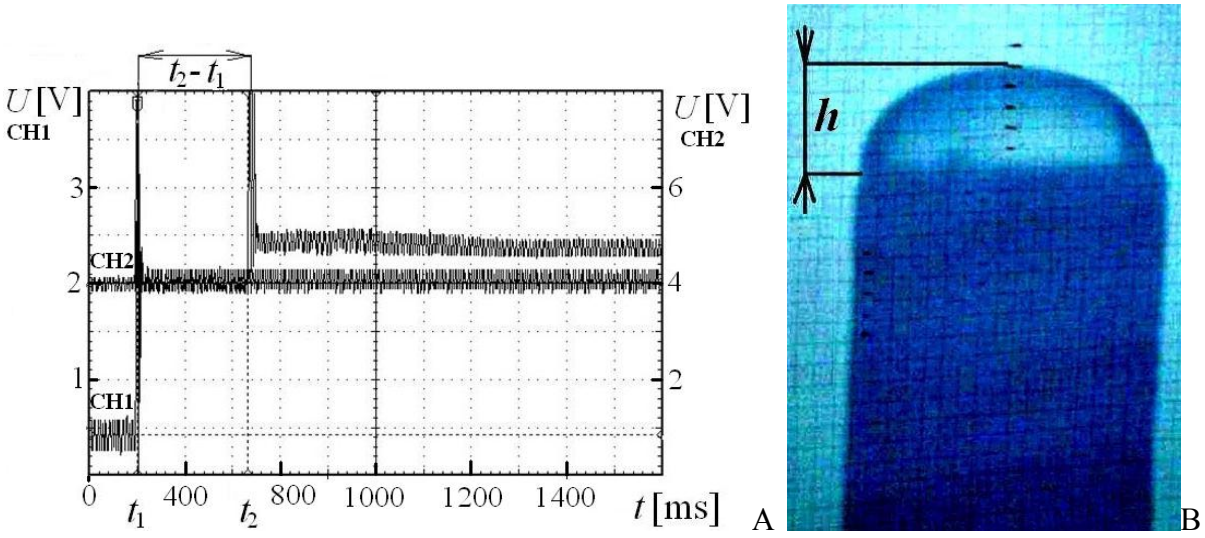

Fig. 2: (A) Oscilloscope records from channels 1 (CH1) and 2 (CH2) provide the time delay $\Delta t = t_2 - t_1$ *between the moments of switching on the field and the onset of jet formation. The potential difference between the spinning electrode and t collector has been set on 12.5 kV in this trial. Voltaic scales differ for CH1 and CH2. (B) A semispherical drop of height h on the top of the spinning electrode.*

First, we observed the behavior of a polymeric droplet deposited with a micropipette atop the rod electrode. The droplet profile was specified from its projection on a screen using the 20x lenses of the stereopticon Meopta, see Fig. 2B. The droplet height *h* was recorded. All experiments were carried out with the droplets having a 1 ml volume. Their height *h* was varied from 3 mm up to 5 mm. The measured delay time corresponded to the droplet transformations from a smooth semispherical shape such as that shown in Fig. 2B to a cusped one shown in Figs. 4 B and C. All experiments were conducted at the ambient temperature 19^0C - 23^0C and relative air humidity changed within 35% - 51%. The stereopticon was switched off after the analyses of the droplet profile and the characteristic hydrodynamic time of the Taylor cone formation was measured.

III. Materials

Experiments were carried out with aqueous solutions of poly (vinyl alcohol) Sloviol-R, purchased from Novacke chemicke zavody, Novaky, Slovakia with molecular weight of 130 000g/mol. Concentrations of tested solutions ranged from 5 wt % up to 15 wt % . Solutions were stirred with a magnetic stirrer Heidolph Vibramax 100 for three hours before each measurement. Surface tension, measured using Krűss tension-meter K121, was recorded for each concentration. To determine the polymeric solution density, 10 ml of the polymer solution was weighed in a Pentometer. All these measurements were repeated 5 times to obtain the standard deviation values.

Tab. 1: Surface tension γ, dynamic viscosity η, density ρ, kinematic viscosity ν and Ohnesorge number of investigated aqueous PVA solutions. The dynamic viscosity was determined for the share rates within the range [50, 600] s^{-1}. All values were measured at temperature of 20°C.

PVA weight concentration in %	Surface tension γ [mN/m]	Dynamic viscosity η [Pa s]	Mass density ρ [kg/m^3]	Kinematic viscosity ν [m^2/s]	Ohnesorge number O_h [-]
5%	43.5 ± 0.1	0.01436 ± 0.00003	994.7 ± 0.6	0.000014455	0.03290
6%	43.5 ± 0.1	0.0174 ± 0.0001	1000.7 ± 0.4	0.000017521	0.06610
7%	43.5 ± 0.2	0.01897 ± 0.00002	1002.3 ± 0.4	0.000018962	0.06618
8%	43.5 ± 0.1	0.0381 ± 0.0001	1003.2 ± 0.3	0.000038114	0.13245
9%	43.5 ± 0.1	0.0532 ± 0.0001	1004.1 ± 0.2	0.000053147	0.16567
10%	43.6 ± 0.1	0.1073 ± 0.0002	1005.4 ± 0.4	0.00010686	0.36420
11%	43.7 ± 0.1	0.1220 ± 0.0001	1005.8 ± 0.5	0.00012139	0.39674
12%	43.7 ± 0.1	0.2008 ± 0.0001	1006.9 ± 0.4	0.00019944	0.62869
13%	43.7 ± 0.1	0.311 ± 0.002	1007.6 ± 0.4	0.00031045	1.02630
14%	43.8 ± 0.1	0.4994 ± 0.0004	1008.5 ± 0.5	0.00049548	1.62052
15%	44.3 ± 0.1	0.5054 ± 0.0004	1009.1 ± 0.1	0.00050109	1.64030

VI. Experimental results

For analysis of experimental data, it is convenient to introduce the following dimensionless parameters characterizing the process of Taylor cone and jet formations:

$$\Gamma = \frac{a\varepsilon E^2}{2\gamma}, \quad a = \sqrt{\gamma/(\rho g)}, \tag{1}$$

where Γ is the dimensionless electrospinning number introduced in Ref. (14) and a is the capillary number, γ is the surface tension, ρ is the liquid density, ε is the dielectric constant of the air, E is the electric field, and g is acceleration due to gravity. The jet is expected to emanate from the Taylor cone when the electrospinning number takes on the critical value $\Gamma_c = 1$. This criticality condition defines the critical field $E_c = \sqrt[4]{4\gamma\rho g/\varepsilon^2}$ which depends only on the physico-chemical parameters of the liquid.

In experiments, the field was not well defined, but the voltage was. The high voltage source was switched on by the switcher, so that the voltage jumped up suddenly to the chosen value. This ensured the most accurate experimental determination of V_C as the lowest voltage for which the liquid surface was destabilized and a jet appeared.

The peak signal from channel 2 was associated with the Taylor cone formation. The characteristic hydrodynamic time was defined as the time delay from the moment of switching on the field to

the appearance of the first peak in channel 2. In order to confirm that the measured time delay is associated with the Taylor cone formation, we employed the high speed imaging with OLYMPUS i-SPEED 3 camera having the frame frequency of 5000 s^{-1}. A rod electrode of 6 mm diameter was used in this series of experiments. With this smaller diameter rod we were able to observe the droplet shape and Taylor cone in the same focal plane. The rod was separated from the counter disk-like electrode by 70 mm gap. The 25 kV voltage was applied to the droplet to observe the Taylor cone formation. .

These experiments suggested that after the Taylor cone formation at the time moment t_2 , the cone started spitting microdroplets or microjets which were detected by the channel 2. Therefore, the time delay measured in experiments can be used for evaluation of the time of Taylor cone formation.

For low-viscous PVA solutions (5% wt) and high electrospinning numbers ($\Gamma = 6$), the time delay was about 24 ms. For highly viscous solutions (15% wt) and subcritical electrospinning number $\Gamma \approx 1$, the time delay increased up to 1269 ms. Time delays Δt's were measured ten times for each concentration and for each value of electrospinning number. A relationship between the experimentally determined dimensionless time delay $T_{Exp} = \Delta t\sqrt{g/a}$ and dimensionless electrospinning number Γ is plotted in Fig. 3 (points). For low electrospinning numbers ($\Gamma \cong \Gamma_c = 1$) we observed only a single jet emanating from the droplet surface. When the electrospinning number increases up to $\Gamma = 6$, we observed 5 jets. The ability to generate

multiple jets with the existing setup can be used for formation of nanofibers in the so-called needleless electrospinning mode (16).

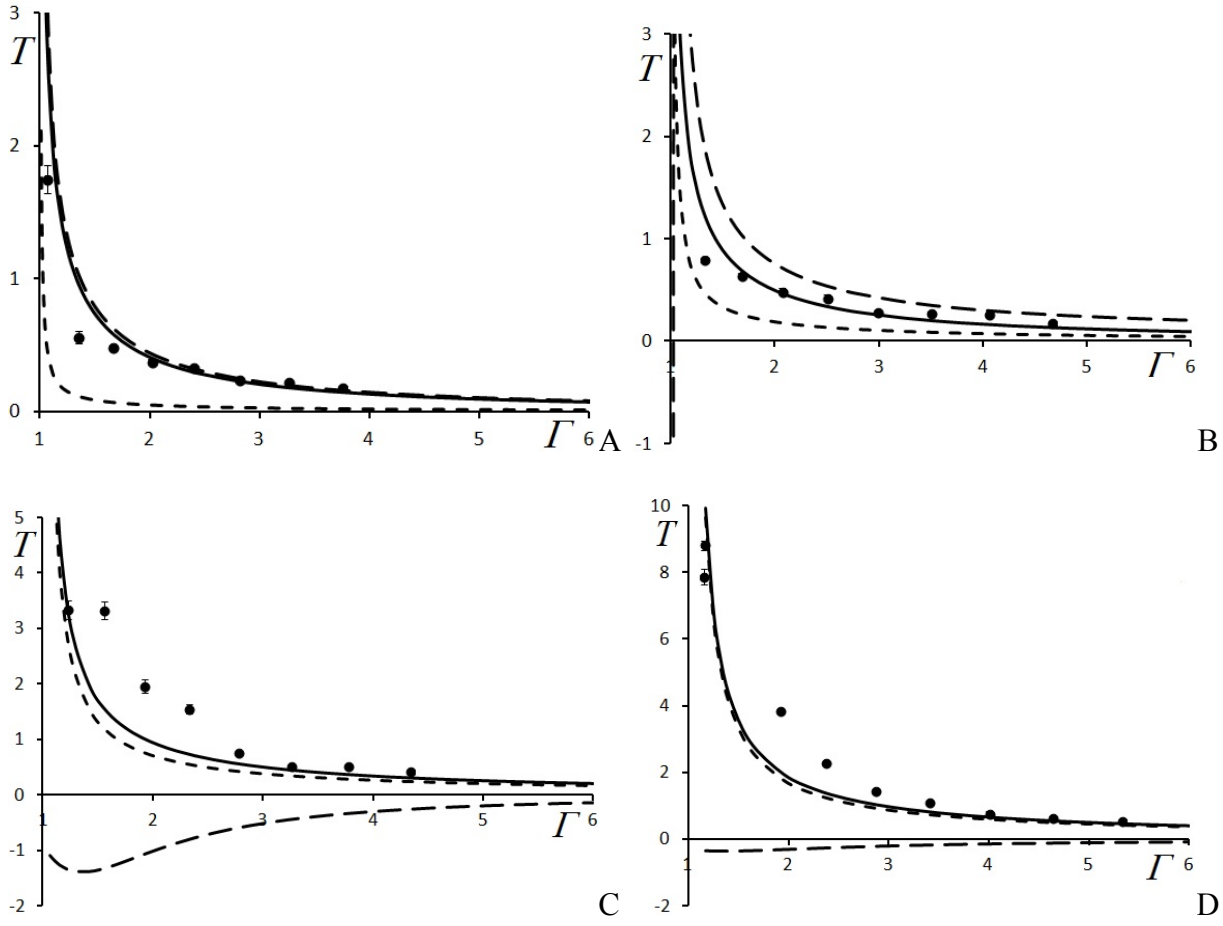

Fig. 3. The time delay T as a function of electrospinning number Γ. Experimental data points correspond to the mean values averaged over 10 measurements each. (A) 5 wt %, PVA solution, O_h=0.033 *(B) 8 wt %, PVA solution,* O_h=0.132 *(C) 12 wt %, PVA solution,* O_h=0.628, *D) 15 wt % PVA solution,* O_h=1.640.

VII. Theoretical interpretation of the time delay

For interpretation of the measured time delays we use the Larmor-Tonks-Frenkel instability theory of the development of ripples on free liquid surfaces (19-21). According to the Larmor-Tonks-Frenkel scenario, a liquid subject to an external electric field ***E*** applied normally to its surface, forms sinusoidal ripples U = A sin (ωt – kx), where U is the vertical displacement of the free surface, and the x-axis is taken in the plane of unperturbed free surface. Assuming that the height of the ripples A is much smaller than the wavelength, Ak << 1, one can employ a linear stability analysis. For conductive incompressible Newtonian liquids with kinematic viscosity ν the relation between frequency ω and wave number k, the dispersion relation, is written as (23, 24, 27) (See supplementary material for derivation of this equation)

$$\left(-i\omega+2\nu k^2\right)^2+\omega_0^2=4\nu^2k^4\sqrt{\frac{-i\omega}{\nu k^2}+1}\,. \qquad (2)$$

where ω_0 is the angular frequency for an inviscid fluid (19-21),

$$\omega_0^2=gk+\frac{\gamma k^3}{\rho}-\frac{\varepsilon_0E^2k^2}{\rho}\,. \qquad (3)$$

An ambient gas is assigned with an electric permittivity ε_0, supposing to be close to the permittivity of vacuum.

In cases of low-viscous liquids and long wavelengths, $-i\omega/\left(\nu k^2\right)>>1$, the solution of the dispersion relation (2) is considered as a small perturbation of the solution ω_0:

$$-i\omega \cong -i\omega_0 - 2\nu k^2 . \qquad (4)$$

In the opposite case of short waves, $-i\omega/\left(\nu k^2\right)<<1$ the linearization of the of the second term on the right hand side of Eq. (2) leads to the approximation $\sqrt{-i\omega/\left(\nu k^2\right)+1} \cong 1-i\omega/\left(2\nu k^2\right)$. This approximation allows one to solve the quadratic equation $\left(-i\omega\right)^2 + 2\nu k^2\left(-i\omega\right)+\omega_0^2 \cong 0$ as (28)

$$-i\omega = -\nu k^2 \pm \sqrt{\nu^2 k^4 - \omega_0^2} \cong -\frac{\omega_0^2}{2\nu k^2}, \qquad (5)$$

where $-i\omega$ is considered real positive for negative ω_0^2. As shown recently (14), formation of jets at free surfaces follows a self-organizing pathway. Once the surface ripples form, they keep evolve and the wave growing faster than others form a cusp followed by emanation of a jet. In terms of the sinusoidal waves with dispersion relation (2), one needs to watch for a root with $-i\omega>0$. The maximum growth rate, i.e. the maximum value $|-i\omega|$, determines the rate of Taylor cone formation. As a characteristic time of the Taylor cone formation, one can choose the reciprocal value of the growth rate, $\tau = 1/\left(-i\omega\right)$.

It is convenient to introduce the following dimensionless complexes

$$\Omega_0^2 = \omega_0^2 \cdot \frac{a}{g}, \quad A = -i\omega\sqrt{\frac{a}{g}}, \quad K = a\,k, \; O_h = \sqrt{\frac{\nu^2}{ga^3}}, \tag{6}$$

where A is the dimensionless growth rate, K is the dimensionless wave number and O_h is the Ohnesorge number. In terms of these dimensionless parameters, dispersion relations (2) – (3) are rewritten as

$$\left(A + 2O_h K^2\right)^2 + \Omega_0^2 = 4O_h^2 K^4 \sqrt{\frac{A}{O_h K^2} + 1}, \tag{7}$$

$$\Omega_0^2 = K^3 - 2\Gamma K^2 + K. \tag{8}$$

Numerical analysis of Eq. (7) is shown in Fig. 3. Fortunately, within the range of experimental parameters, one can significantly simplify Eq.(7) by using the following approximation $4\sqrt{x+1} \cong 2(1+x)$, where $x = A/(O_h K^2)$ (See Supplementary material for numerical confirmation of this approximation). In this approximation, the dimensionless dispersion relation reads $x^2 + 2x + \Omega_0^2/(O_h^2 K^4) = 0$ and its positive solution is written as

$$A = -O_h K^2 + \sqrt{O_h^2 K^4 - \Omega_0^2}. \tag{9}$$

The condition for maximization of the growth rate follows form the anlysis of modified Eq. (9), $f(K,A) = A^2 + 2O_h K^2 A + K^3 - 2\Gamma K^2 - K = 0 : \; \partial f(K,A)/\partial A = 2A + O_h K^2 \neq 0$

$\partial f(K,A)/\partial K = 4O_h AK + 3K^2 - 4\Gamma K + 1 = 0$. The latter together with the requirement $f(K,A) = 0$ leads to $\frac{d\Omega_0^2}{dK} = 2O_h^2 K\sqrt{2\left(K^3 - K\right)}$ (for inviscid fluids it agrees with the known condition $d\Omega_0^2 / dK = 0$ (29)). Analyzing the roots of these two equations, we obtain the relations between the electrospinning number and dimensionless wave number for viscous and non-viscous liquids respectively:

$$\Gamma = \frac{3}{4}K + \frac{1}{4K} + O_h\sqrt{\frac{K^3 - K}{2}}, \qquad (10)$$

$$\Gamma = \frac{3}{4}K + \frac{1}{4K}. \qquad (11)$$

The relation (9) together with the Eqs. (10)-(11) gives the dependence of A on the electrospinning number Γ, for a given Ohnesorge number. These relations enable comparison of the theoretical results with the experimental data on the dimensionless time of Taylor cone formation, T = 1/A:

$$T = 1/\left(-O_h K^2 + \sqrt{O_h^2 K^4 - K^3 + 2\Gamma K^2 - K}\right). \qquad (12)$$

For the critical condition, $A_c = 0$ corresponding to the critical electrospinning number $\Gamma_c = 1$ we obtain the same critical wave number $K_c = 1$ as for the inviscid fluids.

In Fig. 3, each experimental point corresponds to the mean value averaged over 10 experiments. The error bars correspond to the standard deviations. The long-dashed curve corresponds to small viscosity asymptotics, Eq. (4), the short-dashed curve corresponds to the high viscosity case, Eq. (5). More examples of the T-Γ dependences for various polymer solutions can be found in the Supplemental Material [URL inserted by publisher].

VIII. Voltage oscillations

Figures 4A-B demonstrate the correlation between the record from the oscilloscope channel 2 and the growth stages of the Taylor cone obtained on 12 wt % solution of PVA. A video record documenting more details of this relationship is available in the Supplemental Material [URL inserted by publisher]. Figure 4A shows the collector voltage measured on resistor R1. The switch-on signal is not depicted here. This record specifies the features of the signal peak at time t_2 from channel 2, Fig. 2A. Figure 4B collects the selected snapshots from the high-speed movie. As follows from Fig. 4A and Fig. 4B the first sharp peak on the oscilloscope record, B, precedes the jet appearance, since a jet first appears at snapshot J. The first sharp peak, was used to determine the time moment t_2 of the delayed signal in channel 2. This time delay completely characterizes the development of the Taylor cone.

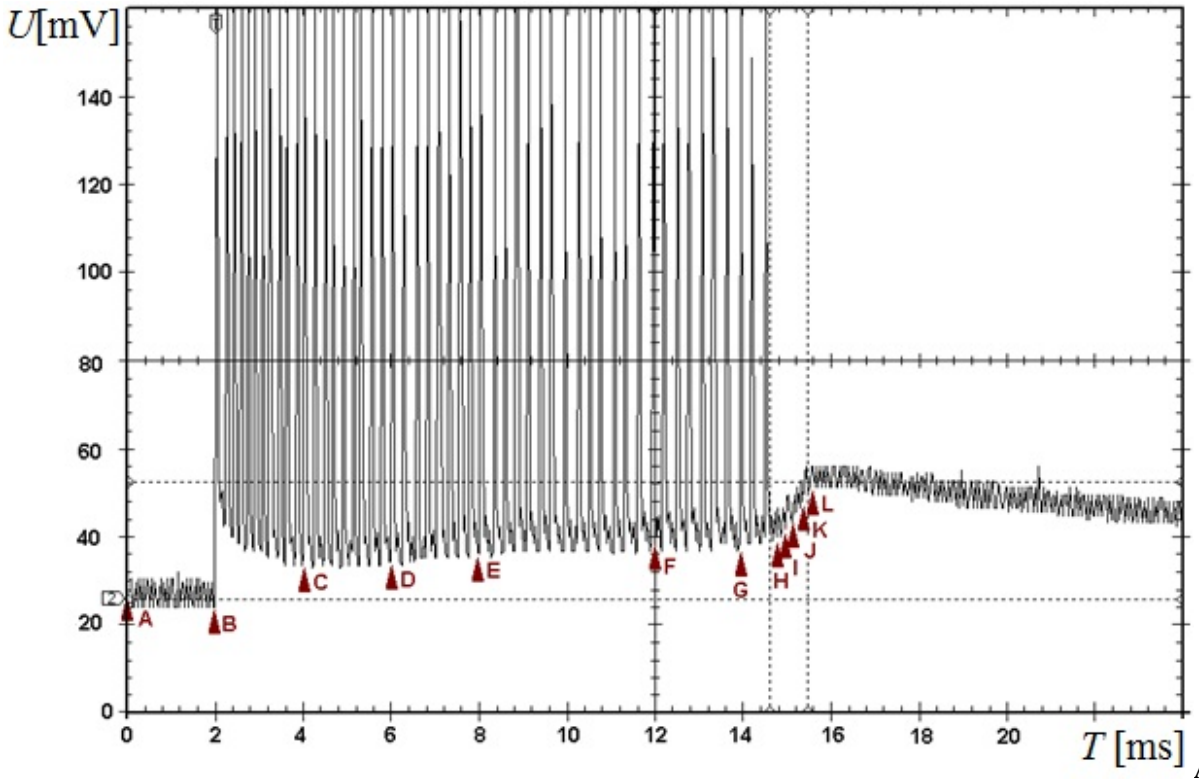
U[mV]
140
120
100
80
60
40
20
0
0
2
4
6
8
10
12
14
16
18
20
T [ms]
A
B
C
D
E
F
G
H
I
J
K
L
A

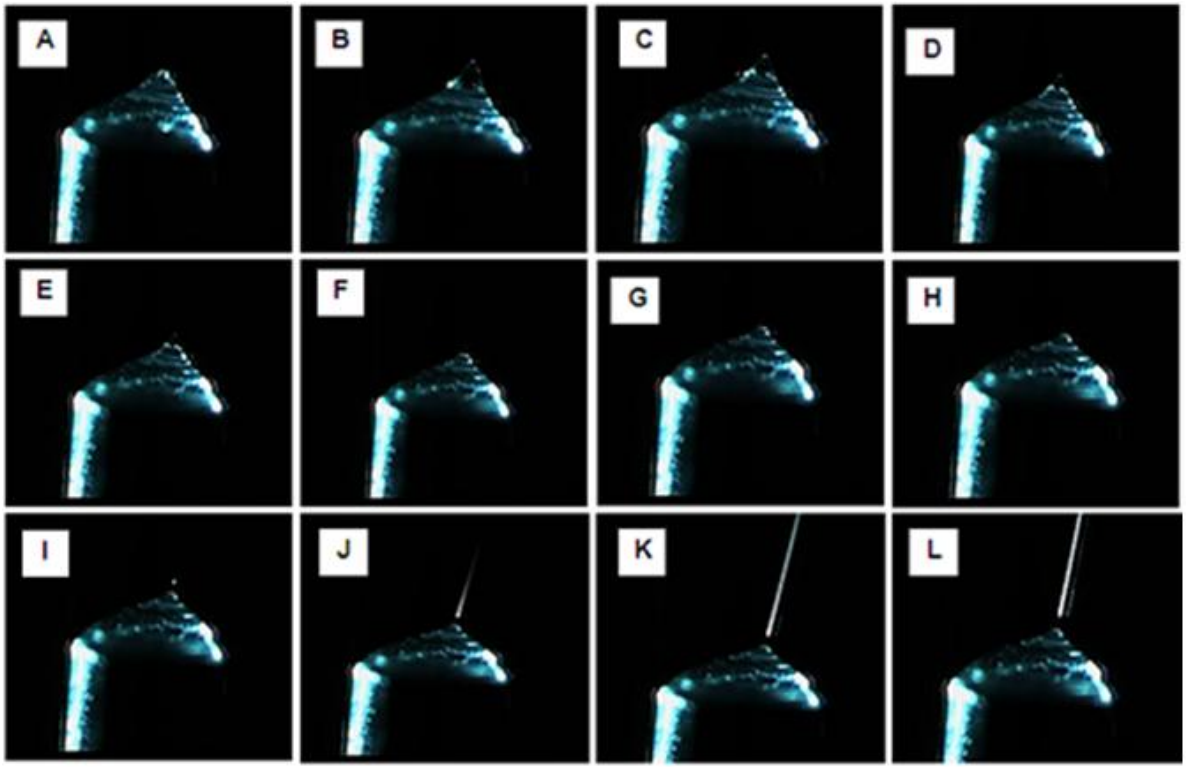
A
B
C
D
E
F
G
H
I
J
K
L
B

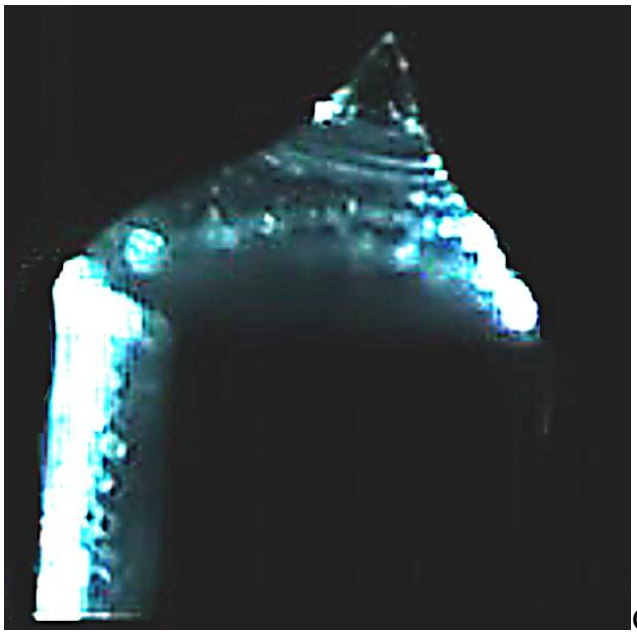 C

Fig. 4. (A) A voltage signal from the oscilloscope channel 2 (CH2) obtained from 12 wt % PVA solution. (B). The sequence of frames taken at the time moments marked in Fig. A. (C) A zoomed picture of the Taylor cone in the snapshot B.

These experiments revealed a new phenomenon occurring prior to the appearance of a jet. This phenomenon comprises a series of discharges in the spinning zone manifested by voltage oscillations. The firs peak on the oscilloscope record from channel 2 is shown in Fig. 4A; it is followed by a series of subsequent peaks corresponding to snapshots C-H in Fig. 4B. The average time delay between these neighboring peaks is 0.24 ms. The origin of these peaks is unknown yet; they can be associated with emission of charged droplets from the Taylor cone. In addition, for high electric fields (above 2.4 MV/m) the air ionization by electron impact can also lead to the voltage oscillations.

The voltage peaks disappeared when the jet was formed. The jet was first observed in image J in Fig. 4B. The jet is present in next snapshots K and L; its formation was accompanied by a monotonous increase of voltage without any voltage oscillations.

These discharges were also studied with droplets of distilled water, Fig. 5A. The voltage peaks are nearly equidistant with the average time delay of 0.48 ms between them. But we were not able to detect any droplet detached from the Taylor cone formed with 12 wt % solution of PVA. The time difference between the peaks on water and polymer solutions is noticeable as well.

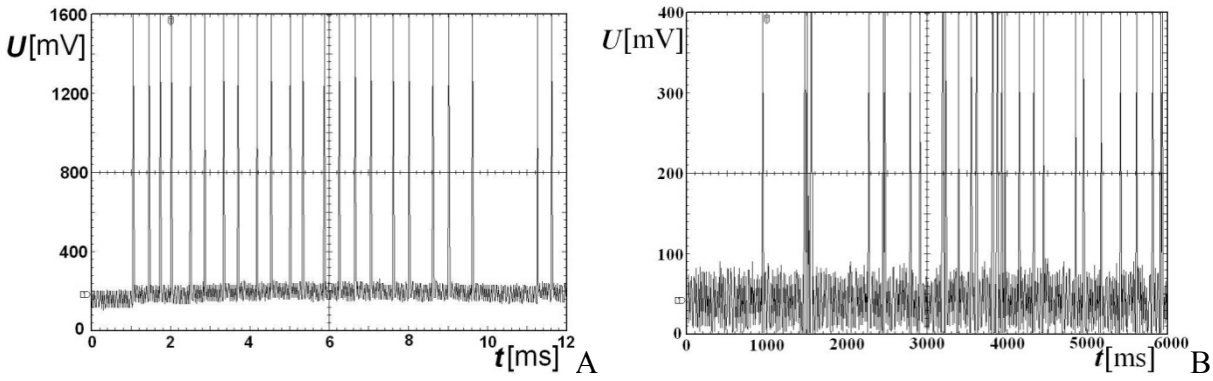

Fig. 5. (A) Oscilloscope record from channel 2 obtained during electrospraying of a distilled water droplet. (B) Oscilloscope record from channel 2 generated by discharges from the bare metallic rod.

In contrast to the periodic peaks on droplets, the discharges from a bare metallic rod are sporadic, Fig. 5B. The mean time delay between subsequent discharges in this case is 203 ms. The differences in regularity and in the mean time delays of signals from the droplets of water, polymer solutions and, bare metallic rod suggest different physical origins of these discharges. These mechanisms are currently under investigation in our groups.

VI. Conclusions

We studied the dynamics of the Taylor cone formation on a surface of a drop subject to an external electric field. Water and aqueous solutions of Polyvinyl alcohol were investigated. We used an experimental setup for the needless electrospinning when a drop in question was placed on a metal rod and a voltage was applied to the rod. The created field was able to withdraw the liquid jets from the droplet surface (14). This setup was equipped with extra circuits and measuring tools to provide accurate measurements of the rod potential relative to the counter electrode-collector and detect flow of charges reaching the collector. The analysis of obtained voltage waveforms showed a time delay between the moment of voltage application and the peak of current associated with arrival of charges to the collector. It was first hypothesized that this current was associated with the first jet emanating from the Taylor cone. However, the high speed imaging with simultaneous analyses of the voltage waveforms showed that a visible micro jet has been formed after the first detection of the arrived charges. This time delay is an order of magnitude shorter than the time delay between the voltage application and the detection of first current peak on the collector electrode. Moreover, a careful inspection of the voltage waveforms measured at the collector revealed the striking difference in the waveforms before and after formation of a stable liquid jet. Namely, some voltage ripples were detected on the collector prior to the signal stabilization when a stable jet has formed. The mechanisms of generation of these voltage ripples is unclear though several scenarios were proposed.

The analysis of the voltage waveforms and images of the drop profiles at different time moments suggest that one can introduce different time scales associated with the electrospinning phenomena. In particular, the characteristic time of the Taylor cone formation can be distinguished from other time scales; this time is correlated with the arrival of the first charges to the collector. It was found that this time depends on polymer concentration, viscosity, and the local electric field in the vicinity of the liquid surface. We have derived the dependence of dimensionless time T of the Taylor cone formation on electrospinning number Γ, Eq.(12). This approximate formula bridges the asymptotic limits known from the literature.

The characteristic time of the Taylor cone formation significantly depends on the liquid viscosity. Remarkably, the effect of polymer rheology seems to be secondary; the results of a model of simple Newtonian fluid fit the experimental data fairy well. Qualitatively, this observation can be explained by the weak tensile and shear stresses developed inside the Taylor cone before the jet emanation.

These results show that the process of fiber electrospinning can be subdivided into stages. The stage of the Taylor cone formation is well separated from other stages. The proposed experimental method of analysis of the characteristic time of Taylor cone formation can also be used for diagnostic purposes to measure the viscosity of polymer solutions or surface tension provided that other parameters are known.

ACKNOWLEDGEMENTS

The authors are very thankful to A. Richter and P. Rydlo from the Technical University of Liberec, for fruitful discussions on experimental setup. D.L., P.M. and P.P. acknowledge the support of GACR, Grant no. P208/12/0105. E.A. and M.B. were supported by the Internal Grant Agency of the Ministry of Health of the Czech Republic Grant no. NT12156 and The Grant Agency of the Charles University Grant no. 384311. L.V. is thankful to the support from The Ministry of Education, Youth and Sports of the Czech Republic via the project "Modification of Nanofibrous Materials by plasmatic technology for biological application" ERA-NET, ME-KONTAKT, CARSILA no. ME10145. R.D. acknowledges the support by BRAIN "Doctoral scholarships as an investment in intelligence" project, financed by the European Social Found and the Romanian Government. The paper was supported in part by the Project OP VaVpI Centre for Nanomaterials, Advanced Technologies and Innovation CZ.1.05/2.1.00/01.0005.

References

1. Katti DS, Robinson KW, Ko FK, & Laurencin CT (2004) Bioresorbable nanofiber-based systems for wound healing and drug delivery: Optimization of fabrication parameters. *Journal of Biomedical Materials Research Part B-Applied Biomaterials* 70B(2):286-296.
2. Du J & Hsieh YL (2009) Cellulose/chitosan hybrid nanofibers from electrospinning of their ester derivatives. *Cellulose* 16(2):247-260.
3. Du J & Hsieh YL (2008) Nanofibrous membranes from aqueous electrospinning of carboxymethyl chitosan. *Nanotechnology* 19(12).
4. Schreuder-Gibson H*, et al.* (2002) Protective textile materials based on electrospun nanofibers. *J. Adv. Mater.* 34(3):44-55.
5. Schreuder-Gibson HL & Realff ML (2003) Advanced fabrics. *Mrs Bulletin* 28(8):558-563.

6. Reukov V, Vertegel A, Burtovyy O, Kornev KG, & Luzinov I (2009) Fabrication of nanocoated fibers for self-diagnosis of bacterial vaginosis *Materials Science and Engineeering C* 29(3):669-673
7. Tsai CC*, et al.* (2011) Nanoporous artificial proboscis for probing minute amount of liquids. *Nanoscale* 3(11):4685-4695.
8. Reneker DH & Yarin AL (2008) Electrospinning jets and polymer nanofibers. *Polymer* 49(10):2387-2425.
9. Rutledge GC & Fridrikh SV (2007) Formation of fibers by electrospinning. *Advanced Drug Delivery Reviews* 59(14):1384-1391.
10. Filatov Y, Budyka A, & Kirichenko V (2007) *Electrospinning of Micro- and Nanofibers: Fundamentals in Separation and Filtration Processes* (Begell House Inc, Redding, CT) p 488 pages.
11. Dzenis Y (2008) Materials science - Structural nanocomposites. *Science* 319(5862):419-420.
12. Ramakrishna S & Teo WE (2006) A review on electrospinning design and nanofibre assemblies. (Translated from English) *Nanotechnology* 17(14):R89-R106 (in English).
13. Reneker DH, Yarin AL, Zussman E, & Xu H (2007) Electrospinning of nanofibers from polymer solutions and melts. *Advances in Applied Mechanics, Vol 41,* Advances in Applied Mechanics), Vol 41, pp 43-195.
14. Lukas D, Sarkar A, & Pokorny P (2008) Self-organization of jets in electrospinning from free liquid surface: A generalized approach. *Journal of Applied Physics* 103:084309.
15. Morton WJ (1902).
16. Yarin AL & Zussman E (2004) Upward needleless electrospinning of multiple nanofibers. *Polymer* 45(9):2977-2980.
17. Miloh T, Spivak B, & Yarin AL (2009) Needleless electrospinning: Electrically driven instability and multiple jetting from the free surface of a spherical liquid layer. (Translated from English) *Journal of Applied Physics* 106(11) (in English).
18. Jirsak O*, et al.* (2005).
19. Frenkel J (1955) *Kinetic theory of liquids* (Dover, New York).
20. Tonks L (1935) A theory of liquid surface rupture by a uniform electric field *Physical Review* 48 (6).
21. Larmor J (1890) On the Influence of Electrification on Ripples. *Proceedings of the Cambridge Philosophical Society. Mathematical and physical sciences.* 7:69-72.
22. Taylor GI & McEwan AD (1965) Stability of a Horizontal Fluid Interface in a Vertical Electric Field. *J. Fluid Mech.* 22:1-&.
23. Melcher JR & Taylor GI (1969) Electrohydrodynamics - a Review of Role of Interfacial Shear Stresses. *Annu. Rev. Fluid Mech.* 1:111-&.
24. Saville DA (1997) Electrohydrodynamics: The Taylor-Melcher leaky dielectric model. *Annu. Rev. Fluid Mech.* 29:27-64.
25. Taylor G (1964) Disintegration of Water Drops in Electric Field. *Proceedings of the Royal Society of London Series a- Mathematical and Physical Sciences* 280(138):383-&.
26. Pokorny P, Mikes P, & Lukas D (2010) Electrospinning jets as X-ray sources at atmospheric conditions. (Translated from English) *Epl-Europhys Lett* 92(4) (in English).
27. Castellanos A ed (1998) *Electrohydrodynamics* (Springer, New York), Vol 380.

28. Levich VG (1962) *Physicochemical Hydrodynamics* (Prentice-Hall, Englewood Cliffs, NJ).
29. Drazin PG & Reid WH (2004) *Hydrodynamic stability* (Cambridge University Press, Cambridge, UK ; New York) 2nd Ed pp xx, 605 p.